CLASS I HISTONE DEACETYLASE INHIBITION AMELIORATES SOCIAL COGNITION AND CELL ADHESION MOLECULE PLASTICITY DEFICITS IN A RODENT MODEL OF AUTISM SPECTRUM DISORDER

Andrew G. Foley, Shane Gannon, Nanette Rombach-Mullan, Alison Prendergast, Claire Barry, Andrew W. Cassidy, Ciaran M. Regan.[1,*]

Berand Neuropharmacology, NovaUCD, Belfield Innovation Park, University College Dublin, Dublin 4, IRELAND.

[1] School of Biomolecular and Biomedical Science, UCD Conway Institute, University College Dublin, Belfield, Dublin 4, IRELAND.

[*] Corresponding author:

Prof. Ciaran Regan

UCD Conway Institute

University College Dublin

Belfield, Dublin 4, IRELAND.

Tel: +353-1-7166775

Fax: +353-1-7166920

E-mail: ciaran.regan@ucd.ie

ABSTRACT

In utero exposure of rodents to valproic acid (VPA), a histone deacetylase (HDAC) inhibitor, has been proposed to induce an adult phenotype with behavioural characteristics reminiscent of those observed in autism spectrum disorder (ASD). We have evaluated the face validity of this model in terms of social cognition deficits which are a major core symptom of ASD. We employed the social approach avoidance paradigm as a measure of social reciprocity, detection of biological motion that is crucial to social interactions, and spatial learning as an indicator of dorsal stream processing of social cognition and found each parameter to be significantly impaired in Wistar rats with prior *in utero* exposure to VPA. We found no significant change in the expression of neural cell adhesion molecule polysialylation state (NCAM PSA), a measure of construct validity, but a complete inability to increase its glycosylation state which is necessary to mount the neuroplastic response associated with effective spatial learning. Finally, in all cases, we found chronic HDAC inhibition, with either pan-specific or HDAC1-3 isoform-specific inhibitors, to significantly ameliorate deficits in both social cognition and its associated neuroplastic response. We conclude that *in utero* exposure to VPA provides a robust animal model for the social cognitive deficits of ASD and a potential screen for the development of novel therapeutics for this condition.

RUNNING TITLE

Social deficit amelioration in rat autism model

KEY WORDS

Histone deacetylase; SAHA; MS-275; social interaction; biological motion; spatial learning; synaptic plasticity; NCAM PSA.

ABBREVIATIONS

HDAC: histone deacetylase; SAHA: suberoylanilide hydroxamic acid; NCAM: neural cell adhesion molecule; PSA: polysialic acid; MS-275: N-(2-amino-phenyl)-4-[N-(pyridine-3-yl-methoxy-carbonyl)-amino-methyl]-benzamide derivative; VPA: valproic acid.

1. INTRODUCTION

The dynamic modification of chromatin complexes by the addition of acetyl groups to core histone proteins by histone acetyltransferases (HATs) and their removal by histone deacetylases (HDACs) provides a mechanism by which genetic and environmental factors may induce phenotypic change over an extended period of time. This has led to the suggestion that altered epigenetic patterning may contribute to the pathophysiology of psychiatric disorders that emerge during development, including autism spectrum disorder (ASD) (Gräff et al., 2011).

ASD is a developmental disorder that arises in approximately 1% of the world-wide population and is comprised of a heterogenous group of conditions characterised by impairments in reciprocal social interactions and the presence of restricted and repetitive and stereotyped behaviours (DSM-IV-TR; American Psychiatric Association, 2006). Although highly heritable, the aetiology of ASD is largely unknown and only 5-15% of cases have an identifiable aetiology (Abraham and Geschwind, 2010). Rett's syndrome, for example, relates to loss of function of the methyl CpG binding protein 2 (*MECP2*) that regulates transcriptional repression through its interaction with methylated DNA and HDAC1 and HDAC2 (Samaco and Neul, 2011). Epidemiological studies have also demonstrated teratogen exposure during the first trimester to be significantly correlated with an increased risk of developing ASD (Christianson et al., 1994; Rasalam et al., 2005). The developmental emergence of this condition has been associated with abnormal synapse remodelling arising from dysregulation of synaptic development proteins, including cell adhesion

molecule function and glycosylation state (Wang et al., 2009; Pinto et al., 2010;), that inexorably gives rise to an array of neuroanatomical malformations (Courchesne et al., 2011).

Despite the improvements in our understanding of the pathophysiology of ASD, progress in the discovery of new therapeutic mechanisms lacks vitality, not least due to the availability of good animal models. Inbred mouse strains, transgenic mouse models and mice with prior teratogen exposure exhibit varying degrees of face and construct validity for one or more of the core deficits observed in ASD (Wagner et al., 2006; Silverman et al., 2010; Peça et al., 2011). Given that genomic variants likely account for 0.5-2% of total ASD cases (Pinto et al., 2010), we were interested to complement existing studies on animal models by determining the extent to which an environmental risk factor might provide face and construct validity. This model employs adult rats of dams which receive a single dose of valproic acid (VPA) at time of neural tube closure (Rodier et al., 1996; Ingram et al., 2000; Schneider and Przewłocki, 2005).

Using this VPA rat model of ASD, we were especially interested to focus on cognition as social reciprocation deficits are a major core symptom of ASD. We also attempted to provide some understanding on the nature of this cognitive phenotype by employing a biological motion paradigm as this has a significant correlation with IQ in human ASD (Rutherford and Troje, 2012). A spatial learning paradigm was employed to account for the consequences of the structural deficits observed in the hippocampus of patients with ASD (Wegiel et al., 2010) as these may contribute to the dorsal stream processing deficits associated with this condition. As a measure of

construct validity, we evaluated cell adhesion molecule function, specifically neural cell adhesion molecule (NCAM) polysialylation (PSA) state, as this has previously been implicated in the pathogenesis of ASD (Plioplys et al., 1990; Purcell et al., 2001). Finally, given the premise that ASDs are linked to epigenetic patterning (Semaco and Neul, 2011) and that covalent modification of core histone proteins has been demonstrated to underpin behavioural modification and synaptic plasticity in adult rodents (Levensen et al., 2004; Guan et al., 2009), we determined the impact of HDAC inhibition on the cognitive and cellular deficits induced by *in utero* exposure to VPA in order to provide confidence in the predictive validity of this model.

2. MATERIALS AND METHODS

2.1. *Animal maintenance*

Experimentally naïve male Wistar rats were purchased from Harlan UK, delivered to the Biomedical Facility at University College Dublin (UCD), housed in groups of 3-4, and maintained under standard laboratory conditions at 22-24 ºC on a 12 hour-light/dark cycle, with food and water available *ad libitum*. Animals were allowed one week to acclimatise to the experimental rooms before any experimental procedures were carried out. All animals were examined and weighed daily. All experimental procedures were approved by the UCD Animal Research Ethics Committee, conformed to EU Council Directive 86–609–EEC, and were carried out by individuals who held the appropriate license issued by the Department of Health.

2.2. *Prenatal exposure of pregnant Wistar rats to valproic acid*

Time-mated female Wistar rats were obtained from Harlan UK, delivered to the UCD Biomedical Facility at gestational day 5, and housed individually under standard laboratory conditions, as described above. The *in utero* VPA rodent model of ASD employed here has been previously described in detail by Schneider and Przewłocki (2005). Briefly, pregnant Wistar rats received a single intra-peritoneal dose of 600 mg/kg VPA (Sigma, UK) (VPA/VEH) in a 1 ml/kg volume of dH_2O on gestational day 12.5 (E12.5). The control dams received a single similar volume injection of dH_2O at the same gestational time-point (VEH/VEH). All animals exposed to VPA during gestation developed a characteristic 'kink' in the tail (Vorhees, 1987), which was easily distinguishable from aged-matched controls and used to confirm successful

exposure to the teratogenic actions of VPA (Figure 1A). Litters were closely observed for other teratogenic effects following *partem* (Figure 1B), standardised to n=8 per litter (maximising the number of males) and then left undisturbed until the time of weaning on postnatal day (P) 25 when the male off-spring were housed in groups of 3-4, as described above, until behavioural testing commenced on P72.

2.3. *Behavioural analysis*

Two separate experimental protocols were carried out in this study. The first study assessed propensity for social interaction and spatial learning ability in cohorts of animals with prior exposure to VPA (Figure 2A). The second experimental group was used to evaluate the perception of biological motion as detailed in Figure 2B. Prior to all behavioural analyses, animals were transferred and housed in the experimental rooms within the animal husbandry facility on P67 for a period of 5 days. Experimental analyses were carried out before 12.00h to minimise the influence of circadian rhythm on behaviour.

2.4. *Drug dose and route of administration*

Studies were conducted using suberoylanilide hydroxamic acid (SAHA; Axxora Ltd. UK, batch number L15566), a pan-specific HDAC inhibitor, and the benzamide 4-[[(2-aminophenyl)amino]carbonyl]-phenyl]methyl]-3-pyridinylmethyl ester carbamic acid (MS-275; Axxora Ltd. UK, batch number L14358/a) which specifically inhibits HDAC 1-3 isoforms (Bolden et al., 2006). The structures of these compounds are shown in Figure 2C. SAHA was administered via the intraperitoneal route (i.p.) at 5 mg/kg in a 2 ml/kg dose volume of a 2-hydroxypropyl-beta-cyclodextrin vehicle (9 g/L). MS-275 was administered i.p. at 1 mg/kg in a 2 ml/kg dose volume of dH_2O

vehicle (solubility was assisted by first dissolving the MS-275 with a drop of 100% glacial acetic acid and adjusting the pH to 6.6 by the addition of NaOH). Vehicle-treated controls were employed for comparison to each experimental cohort. In the first experimental protocol the cohorts of VPA-treated animals received either 5 mg/kg SAHA (VPA/SAHA) or 1 mg/kg MS-275 (VPA/MS-275) for 8 days prior to and on each day during behavioural analysis (administered 1 hour pre-training), a total of 21 days drug exposure. Comparison was made to vehicle-treated offspring from dams that had received VPA (VPA/VEH) or vehicle (VEH/VEH) *in utero*. In the second experimental protocol the VPA-treated animals received the drug for 16 days prior to training and on each of the 5 daily sessions in the training phase, a total of 21 days treatment. The temporal sequence of drug administration in relation to behavioural analysis is shown in Figure 2A and B. The drug doses employed were based on previously published data (Alarcon et al., 2004) and on in-house range finding experiments (data not shown).

2.5. *Social approach-avoidance paradigm*

2.5.1. *Apparatus*

The social-approach avoidance paradigm was adapted from a previously published procedure that had been developed for mice (Brodkin et al., 2004). In essence, the paradigm employed assessed the propensity of the test Wistar rat to approach and associate with an unfamiliar, experimentally naive stimulus rat of the same strain, equal size (weight) and age, and unrelated to the animals of the experimental cohorts. This behavioural response was evaluated in a rectangular box (65 cm long x 30 cm wide x 35 cm high) constructed of black Perspex and containing two identical chambers (10 cm long x 30 cm wide x 35 cm high) at either end. These chambers

were separated from a central area by clear Perspex sheets with multiple, small, evenly spaced holes over the entire wall (Figure 3A). The central portion of the apparatus contained two black Perspex baffles that provided a 10cm space between the end of the baffle and outer wall of the apparatus. These baffles created three equally sized and interconnected areas (15 cm long x 30 cm wide x 35 cm high). The test animal was placed between these baffles at the start of each trial and allowed to interact with the stimulus animal (randomly placed in either the left or right chamber) through the holes in the clear Perspex that permitted auditory, visual and olfactory interactions. Both stimulus and test animals were housed under identical conditions, as described above, until time of assessment. In all cases the stimulus animal was a drug-naïve and the test animal had been exposed to vehicle *in utero* (VEH/VEH), VPA *in utero* (VPA/VEH), or exposed to VPA *in utero* and later treated with HDAC inhibitors (VPA/SAHA or VPA/MS-275).

2.5.2. *Behavioural assessment*

At the beginning of each trial the entire apparatus was cleaned with 70% ethanol, dried and fresh sawdust bedding material added. The test animal was placed between the black Perspex baffles of the central area from which it could move to freely explore all areas of the apparatus during a 5-minute acclimatisation period. Exploratory behaviour was monitored using an overhead video camera linked to Ethovision XT (Noldus, UK) tracking software. Time spent in each area was recorded when both head and forelimbs were within the circumscribed social, centre, and non-social areas. Following the completion of the acclimatisation period the test rat was removed to a holding cage, the bedding material was redistributed and a stimulus animal placed in one of the side chambers, subsequently designated the

social area. A different naïve stimulus animal was paired with every test animal. The test animal was returned to the central area and the time spent in each of the three areas was again recorded for a 5-minute period. In addition, the total time engaged in social interactive behaviour, such as nose-poking and paw-reaching activity, at the separating baffle was recorded for each treatment group.

2.5.3. *Data analysis*

The total amount of time spent in each chamber of the apparatus was calculated and expressed as the mean ± SEM for both acclimatisation and test phases of the paradigm and the presence of significant bias for a particular chamber was determined by one-way ANOVA for each treatment group. Significant differences between drug treatment and the amount of time animals spent in a specific chamber were determined by two-way ANOVA followed by *post-hoc* Bonferroni analysis. Total time engaged in active social behaviour was determined for each treatment group and analysed by Mann-Whitney U-test. A social approach-avoidance score, defined as the time spent in the social chamber minus time spent in non-social chamber, was determined for each treatment group and analysed by Mann-Whitney U-test. In all cases, values of $p<0.05$ were deemed to be significant.

2.6. ***Biological Motion Perception Paradigm***

2.6.1. *Apparatus*

The experimental design employed a touch-screen cognitive testing method that was based on previously published work (Bussey et al., 2008). Training and behavioural testing were carried out in a semi-automated testing apparatus constructed by using a modular testing chamber (30 cm long x 24 cm wide x 8 cm high; Med Associates Inc.,

USA) consisting of a metal frame, clear Perspex walls, and a stainless steel grid floor (Figure 4A). A food magazine was located at either end of the chamber and attached to a pellet dispenser secured to the outside of the box. The food dispensers were designed to deliver a single standardized 45 mg food pellet (Med Associates Inc., USA) into the food magazine coincident with its illumination by a 3 W white light bulb. The food magazine was fitted with photocell capable of detecting a rat nose poke. A flat-screen LCD monitor (10.5 cm high x 6.7 cm wide; Craft Data Ltd., UK) was fitted above each food magazine and the chamber was also fitted with two 3W white lights and a tone generator (Med Associates Inc., USA).

2.6.2. *Behavioural assessment – Pre-training phase*

Rats, restricted to an 85% free-feeding weight, were initially allowed to freely retrieve food pellets placed in the food magazine by remote control during a 10 minute habituation session. In the following session, 24 hours later, the rats were trained to nose-poke the magazine to retrieve a food pellet and its delivery was paired with the illumination of the magazine light and presentation of a tone (65 dB, 1 s). The next stage of training, on the following day, required the animal to respond to various visual stimuli (to avoid the development of bias) presented simultaneously for 30 seconds on both screens in the chamber. These stimuli consisted of a series of white shapes (circles, squares, triangles) on a black background that were initially static before moving from top to bottom of the screen over a 5 second period. A single pellet was delivered immediately after presentation of the stimulus, however, a nose-poke during stimulus presentation resulted in a reward of two pellets and the stimulus was extinguished immediately. Rats were removed from the testing chamber after 15 minutes regardless of the number of trials completed.

Rats were next required to respond to the stimulus presented in one of the two response screens. The stimulus remained on the screen until the rat responded to it whereupon the magazine became illuminated, a reinforcement tone sounded and a food pellet was delivered. This was followed by an interval of 10 seconds before the stimulus for the next trial was displayed. Rats were required to successfully complete 20 trials in a 15 minute session before proceeding to next phase of autoshaping. This following stage of training required the animal to distinguish and approach the screen showing the stimulus in order to obtain the food pellet by a nose-poke in the magazine located below the screen. Correct responses resulted in the disappearance of the stimulus, illumination of the food hopper, tone presentation and delivery of a food pellet. An incorrect response resulted in the disappearance of the stimulus and extinction and the chamber light for a 5 second period. Each trial was separated by a 10 second interval and trials were repeated until the rat made a correct single choice before the random presentation of both stimuli for the next training phase. The final pre-training stage required the animal to discriminate between two distinct stimuli presented simultaneously on both screens using the same response criteria described for the previous training phase.

2.6.3. *Behavioural assessment – Testing phase*

Once autoshaping was complete, the ability of the rats to discriminate between a point-light display of biological motion, white dots moving on a completely dark background (a walking hen; open-access video source from Vallortigara et al., 2005) (Figure 4A), and one of four manipulations of that pattern (static, inverted, scrambled, and rotating versions of the pattern) was determined using the procedures outlines

above. Presentation of correct (directed biological motion) and incorrect manipulated stimuli on the screens was pseudo-random as a given stimulus could not appear on the same screen for more than three consecutive trials. Performance was measured by calculating the percent correct choices in a session that included 20 trials.

2.6.4. *Data analysis*

Performance of the animals in the biological motion paradigm was expressed as a percentage of correct choices with values significantly different between experimental groups being analysed by two-way ANOVA and the Mann–Whitney U-test for non-parametric data. In each case, a p-value less than 0.05 was considered to be significant.

2.7. ***Water maze spatial learning paradigm***

2.7.1. *Apparatus*

The water maze spatial learning paradigm was carried out as previously described (Murphy et al., 1996). Briefly, the water-maze apparatus consists of a circular pool (1.5 m diameter, 80 cm high) with a platform (11 cm diameter) submerged 1.5 cm below the water surface in one quadrant of the maze, 30 cm from the sidewall. Both the pool and platform are constructed from black Perspex and offered no intra-maze cues to guide escape behaviour. By contrast, the training room contained several obvious extra-maze visual cues to aid the spatial orientation necessary for escape learning. The water of the maze temperature was maintained constant at 26±1 ºC by a hidden heating element at the bottom of the pool and a pump was used to circulate the water.

2.7.2. *Behavioural assessment*

The water-maze paradigm consisted of both acquisition and recall components. During acquisition, each trial started with the rat placed facing the wall of the maze at one of three designated locations. Animals were then allowed to freely explore the maze and the time taken to find the hidden platform within a 90-second criterion period was defined as the escape latency time. On the first trial only, rats failing to locate the platform within the 90-second period were guided to it and placed on it for 10 seconds. Escape latencies were measured over 5 trials in each daily session and an inter-trial rest interval of 300 seconds was allowed. Animals were trained in daily sessions over 4 days. Recall of platform position was assessed by a probe test at 24 h (P86) and 72 h (P88) following the final training session. During the probe test the platform was removed and animals were allowed to explore the maze for 30 seconds. The time spent in each quadrant was recorded and used to compare recall of the original position of the platform.

2.7.3. *Data analysis*

Swim behaviour in the water-maze paradigm was monitored using Ethovision XT (Noldus, UK). All data were calculated as mean ± SEM for all trials of all sessions and the presence of significant difference between treatments was determined by two-way ANOVA and *post-hoc* Bonferroni analysis of the data set. In all cases, values of $p<0.05$ were deemed to be significant.

2.8. ***NCAM PSA Immunolabelling***

Tissue preparation and sectioning

Freshly dissected rat brains were split and each half was coated in optimum cutting temperature (OCT) compound and lowered into a Cryoprep freezing apparatus containing dry-ice-cooled n-hexane. The combination of the OCT compound and n-hexane was used to ensure even freezing of the tissue and avoid freezing artefacts. The immunohistochemical procedures employed to detect NCAM PSA have been described in greater detail previously (Fox et al., 1995a). Briefly, horizontal frozen brain sections (12 μm) were cut on a Microm Series 500 cryostat at -15 ºC. All sections were prepared on the day of the experiment and were not pre-cut and stored frozen. For the analysis of the NCAM PSA-positive hippocampal dentate granule cell layer/hilus border cells 10 alternate sections were taken at a level equivalent to -5.6mm below bregma (Paxinos and Watson, 2007). Cryosections were thaw-mounted onto glass slides and immersion fixed for 30 minutes with 70% (v/v) ethanol and incubated overnight with anti-PSA monoclonal antibody (Chemicon, UK) diluted 1:500 in 0.1 M PBS containing 1% (w/v) bovine serum albumen (BSA) and 1% (v/v) normal goat serum (NGS). The sections were exposed for 3 hours to FITC-conjugated goat anti-mouse IgM diluted 1:100 (Calbiochem, UK), again in PBS containing 1% BSA and 1% NGS, and mounted in Citifluor (Agar, UK).

2.8.2. *Quantitative evaluation of NCAM PSA expression*

Quantitative image analysis was performed using Axiovision (Zeiss, UK) a PC-based software package connected to a Leitz DM RB fluorescent microscope with a high sensitivity CCD video camera. The total number of NCAM PSA-immunoreactive neurons in the dentate granule cell layer/hilar border were counted in 6 alternate 12 μm sections commencing -5.6 mm from bregma (Paxinos and Watson, 2007), to

preclude double counting of the 5-10 μm perikarya. Cell identification was aided by the use of the nuclear counter-stain propidium iodide (40 ng/ml PBS; 60 seconds). Cell counts were standardised to unit area of the granule cell layer, 0.15 ± 0.01 mm^2 at this level, and expressed as mean ± SEM values. Statistical analysis employed the Student's t-test and values of $p<0.05$ were deemed to be significant.

2.8.3. *Learning dependent activation of NCAM PSA*

The frequency of polysialylated NCAM immunopositive neurons in the dentate gyrus has been repeatedly shown to be increased 12 hours following acquisition of spatial learning and conditioned avoidance tasks (Fox et al., 1995a; Murphy et al., 1996). In a separate experimental cohort, VPA-exposed rodents and vehicle controls animals (n=6), as well as a separate cohort of VPA-exposed animals treated with MS-275, were subjected to the initial 5 trial training session outlined in the water-maze spatial learning paradigm. Animals were then sacrificed 12 hours following the completion of the last trial, the brains excised and processed for immunolabelling of NCAM PSA as described above. Separate cohorts of all experimental groups were employed as passive naive controls, briefly animals were allowed to explore the water maze in the absence of the hidden platform for the same interval as their trained counterparts. Passive controls were then sacrificed 12 hours following completion of the last trial of the training session and processed for NCAM PSA immunofluorescence staining and analyzed as described above.

3. RESULTS

3.1. *VPA-induced developmental deficits*

All animals exposed to VPA *in utero* exhibited a 'tail kink', as has been described previously in rats following administration of VPA (Vorhees, 1987), and this deformity was used to confirm successful exposure to the teratogen (Figure 1A). In addition, a delay in eye-opening was observed in the VPA-treated animals (Figure 1B) which may be attributable to the impaired/delayed craniofacial nerve development that is typical in this animal model of ASD (Rodier et al., 1996; Tashiro et al., 2011). No other gross developmental abnormalities were observed in VPA-exposed animals. Litter size and male to female sex ratio was unaltered and weight gain was unimpaired over the time period examined (Figure 1B).

3.2. *Social cognition: Social approach avoidance paradigm*

Deficits in social reciprocation, a core feature of ASD (American Psychiatric Association: DSM-IV-TR , 2006), were examined in rats with prior *in utero* exposure to VPA using a social approach-avoidance paradigm, adapted from that described previously for mice (Brodkin et al., 2004). During the acclimatisation phase of the paradigm both vehicle-treated and VPA-exposed cohorts exhibited no preference for any chamber and spent equal amounts of time exploring all areas of the apparatus ($F[2,23]=0.03$ and 2.34, $p=0.97$ and 0.12, vehicle and VPA-treated, respectively). The introduction of a stimulus rat into either the left or right chamber resulted in the vehicle-treated animal showing an increased tendency to interact socially, however, the amount of time spent in the social area did not achieve significance ($F[2,23]=2.833$; $p=0.783$) (Figure 3B). In contrast, the VPA-treated animals

displayed a clear avoidance of the stimulus rat showing a significant bias for the non-social area ($F[2,23]=11.55$; $p=0.0004$) and spending approximately 50% less time investigating the stimulus rat as compared to the vehicle-treated rat ($p=0.0281$; Mann-Whitney U-test) (Figure 3B). These differences could not be attributed to any behaviour in the stimulus animal as their exploratory activity was unchanged when exposed to either vehicle or VPA treated test animals (8.9±0.8 m vs 8.4±0.7 m; distance traveled/5 min) and a different naïve stimulus animal was paired with each test animal. The marked asociality exhibited by VPA-treated animals was further underlined by the significant reduction in the approach-avoidance score ($p=0.0104$; Mann-Whitney U test) and time engaged in social behaviour ($p=0.0011$; Mann-Whitney U test), as compared to the vehicle-treated cohorts (Table 1).

The social cognition deficits observed in the VPA-treated animals could be reversed by treatment with HDAC inhibitors. Treatment of VPA-exposed animals with the pan-specific HDAC SAHA inhibitor or the class I HDAC inhibitor MS-275 was without effect on the time spent exploring the individual areas of the apparatus during the acclimatisation phase of the paradigm (data not shown). However, treatment of VPA-exposed cohorts with SAHA (5 mg/kg) resulted in a significant amelioration of the social deficits observed in the vehicle-treated VPA cohorts following the introduction of a stimulus rat ($F[2,23]=26.14$; $p<0.0001$) (Figure 3B). Moreover, this enhancement of social cognition in the VPA-treated animals was restricted to inhibition of one or more of the HDAC 1-3 isoforms as precisely the same effect was observed with MS-275 (1 mg/kg) ($F[2,23]=13.58$; $p<0.0002$), an HDAC inhibitor which specifically inhibits these isoforms (Figure 3B). Treatment with both SAHA and MS-275 resulted in VPA-treated cohorts spending an equal amount of time

investigating the stimulus rat as compared to their vehicle control counterparts (VEH/VEH) ($F[2,23]=0.0620$; $p=0.9395$) (Figure 3B), a 2-fold increase in approach-avoidance scores ($p=0.0002$ and $p=0.0002$, respectively; Mann-Whitney U-test) and a significant increase in total time actively engaged in social behaviour ($p=0.0011$ and $p=0.0006$, respectively; Mann-Whitney U-test) (Table 1).

In order to determine if HDAC inhibition had a direct action on the enhancement of social cognition we determined the effect of SAHA and MS-275 in normal animals. Administration of either SAHA (5 mg/kg) or MS-275 (1 mg/kg) resulted in the treated animals spending significantly greater lengths of time exploring the stimulus animal in the social chamber ($F[2,17]=60$; $p<0.0001$ and $F[2,17]=52.7$; $p<0.0001$, respectively). Further, treatment with 5 mg/kg SAHA significantly increased the amount of time animals spent in investigating the stimulus rat ($p=0.015$; Mann-Whitney U-test), an effect also observed when the approach-avoidance score was analysed ($p=0.027$; Mann-Whitney U-test). Likewise, MS-275 significantly enhanced the sociality of Wistar rats during the training phase of the paradigm, as compared to their vehicle-treated controls, improving both the amount of time animals spent in the designated social chamber ($p=0.0043$; Mann-Whitney U-test) and the approach-avoidance score ($p=0.0043$; Mann-Whitney U-test).

3.3. *Social cognition: Biological motion perception paradigm*

As the above social approach avoidance paradigm can serve only as a proxy for the more complex pattern of affiliative behaviour that is disrupted in ASD, we further probed malfunctioning in the processing of perceptual stimuli in rats following *in utero* exposure to VPA. For this analysis, we developed a paradigm that measured

orientation to point light displays of biological motion using the touch-screen cognition testing method as described by Bussey and colleagues (2008). Biological motion is a highly robust detection signal that emerges in early development and is crucial for social interactions (Blake and Shiffrar, 2007). Control animals autoshaped to respond to this biological motion detection task exhibited a consistent performance over the 5 training sessions of 20 trials per day with the fraction of correct choices being in the range of 0.6-0.7 (Figure 4B). Animals with prior *in utero* VPA exposure similarly exhibited a constant performance over the 5 training sessions however their fraction of correct choice of the biologically relevant stimulus was significantly lower than that observed in the control animals and was in the range of chance performance of 0.5 ($F[1,90]=27.04$; $p<0.0001$). This deficit in biological perception was ameliorated by chronic HDAC inhibition. Administration of SAHA (5 mg/kg) for 16 days prior to training, and prior to each training session, significantly improved performance as compared to that observed in the VPA/VEH animals ($F[1,90]=4.35$; $p=0.0399$). This drug-induced reversal of the deficit was not complete, however, as the VPA/SAHA group remained significantly impaired as compared to the control animals (VEH/VEH) ($F[1,90]=8.59$; $p=0.004$).

3.4. *Social cognition: Spatial learning paradigm*

As the biological motion deficits associated with ASD have been suggested to reflect a more widespread dysfunction within the dorsal stream of cognitive processing (Spencer et al., 2000; Milne et al., 2005), we determined if animals with prior *in utero* exposure to VPA were impaired in spatial learning as this function is dependent on the dorsal aspect of the hippocampus (Moser et al., 1993; Maguire et al., 2000). All experimental groups employed readily acquired the position of the hidden platform

during the training phase of the water-maze paradigm ($F[3,617]=94.00$; $p<0.001$, two-way ANOVA). However, cohorts administered VPA *in utero* were significantly slower at reaching the target platform than vehicle-treated controls across all four training sessions ($F[1,56]=18.15$; $p<0.0001$) and this impairment was particularly evident during session 4 **(**$p<0.05$; Bonferroni *post-hoc* t-test**)** (Figure 5A**).** The impairment in task acquisition displayed by VPA-treated animals was not the result of slower swim speeds but a failure to implement an adequate search strategy as the path length of these animals was significantly longer than that observed for the vehicle controls **(**$F[1,56]=11.77$; $p<0.001$, two-way ANOVA**)** (Table 2). Furthermore, retention of platform position was significantly disrupted in VPA-exposed cohorts as, during the 24 hour probe trial, animals spent approximately 25% of time in the target quadrant performing just above chance level (Figure 5B). This is in stark contrast to control cohorts that spent a significant longer period of time in the target quadrant ($p=0.0345$; unpaired Student's t-test). Recall of the platform position was also poor in the 72 hour post-training probe trial during which the VPA-treated animals spent less than 20% of time in the target quadrant (Figure 5B). It should be noted, however, that previous studies employing the VPA model of autism have failed to detect any deficits in rat spatial learning (Markram et al., 2008).

The ability to ameliorate the learning deficits in the VPA-exposed animals was investigated using the pan-specific HDAC inhibitor SAHA and compared to the effects obtained with MS-275, a HDAC inhibitor specific to the HDAC1-3 class I isoforms of which HDAC2 and HDAC3 have been demonstrated to negatively regulate memory formation (Guan et al., 2009; Kilgore et al., 2010; McQuown et al., 2011). Treatment of VPA-exposed cohorts with the broad spectrum and class I

specific HDAC inhibitors, SAHA and MS-275, significantly reversed the deficits in both acquisition and recall of the water-maze task. During the acquisition phase VPA-treated cohorts treated with either 5 mg/kg SAHA ($F[1,56]=25.44$; $p<0.0001$, two-way ANOVA) or 1 mg/kg MS-275 ($F[1,56]=45.93$; $p<0.0001$) displayed significantly reduced escape latencies over the 4 training sessions compared to VPA-treated controls (Figure 5A). This enhancement in acquisition was particularly evident on session 2 ($p<0.05$, Bonferroni *post-hoc* t-test), session 3 ($p<0.05$, Bonferroni *post-hoc* t-test) and session 4 ($p<0.05$, Bonferroni *post-hoc* t-test). The significant reduction in escape latency exhibited by SAHA ($F[1,56]=15.67$; $p<0.0001$, two-way ANOVA) and MS-275 ($F[1,56]=27.64$; $p<0.0001$, two-way ANOVA) treated cohorts was a consequence of animals employing a more robust search strategy rather than the product of increased swim speeds across the training sessions (Table 2). Moreover, this enhancement in task acquisition significantly improved the recall of the platform position during recall probe trials, as animals treated with 5 mg/kg SAHA and 1 mg/kg MS-275 spent approximately 50% and 55% of time searching the target quadrant 24 hours post-training and this level of retention was maintained above 40% in both treatment groups during the 72 hour post-training trial (Figure 5B).

The effect of HDAC inhibition on water maze acquisition and recall was also evaluated in normal animals in which chronic administration of either 5 mg/kg SAHA or 1mg/kg MS-275 significantly reduced the escape latencies of Wistar rats ($F[1,40]=22.6$ and 8.4; $p<0.001$ and $p=0.006$, respectively) during task acquisition. Retention of the platform position during probe trials was also significantly improved following HDAC inhibitor treatment with all groups exhibiting robust recall at the 24

hour probe trial. However, at the 72 hour probe time, both SAHA and MS-275 treatment significantly enhanced task retention ($p<0.05$; Mann-Whitney U-test).

3.5. *Influence of HDAC inhibition on spatial learning and social interaction in normal animals*

The possibility that amelioration of the cognitive and social deficits in the ASD model might be attributed to an indirect action of the HDAC inhibitors, we determined the effect of SAHA and MS-275 on the behavioural phenotype of normal Wistar rats. We also evaluated the effect of VPA on these parameters in order to determine if its ability to inhibit HDAC produced similar effects to those obtained with SAHA and MS-275.

All cohorts employed in the water-maze paradigm readily acquired the position of the hidden platform over the 4 training sessions and chronic administration of SAHA (5 mg/kg) significantly reduced the escape latencies ($F[1,40]=22.6;p<0.001$). This was particularly evident during the initial two sessions, as judged by Bonferroni post t-tests ($p<0.05$) (Figure 6A). Administration of the class I specific HDAC inhibitor MS-275 (1 mg/kg) similarly resulted in improved spatial learning, as judged by significant reductions in escape latency over the four training sessions compared to vehicle treated controls ($F[1,40]=8.4$; $p=0.006$) (Figure 6B). VPA (150 mg/kg) similarly enhanced acquisition of the spatial learning paradigm ($F[1,40]=8.2$; $p=0.0065$) (Figure 6C), however, this HDAC inhibitor failed in the successful consolidation of the task, as judged by the complete lack of recall of platform position in the 72 h probe test (Figure 6D). This contrasted sharply with the significant recall of platform position observed in animals following chronic administration of either

SAHA or MS-275 ($p<0.05$; Mann-Whitney U-test) (Figure 6D). Moreover, no significant difference was observed in the average swim speed of animals treated with either SAHA, MS-275 or VPA, as compared to their vehicle-treated counterparts (data not shown).

In the social approach avoidance paradigm, introduction of a stimulus animal into the chamber failed to result in the vehicle-treated control animals to display a preference for the designated social chamber ($F[2,17]=2.00$; $p=0.12$, one-way ANOVA). However, chronic administration of animals with SAHA resulted in significant preference for the social chamber ($F[2,17]=60$; $p<0.0001$, one-way ANOVA) in which they spent a significantly increased amount of time investigating the stimulus rat ($p=0.015$; Mann-Whitney U-test) (Figure 6E). Chronic treatment with MS-275 similarly enhanced the animals preference for the social chamber ($F[2,17]=52.7$; $p<0.0001$; one-way ANOVA) and time engaged with the stimulus rat ($p=0.0043$; Mann-Whitney U-test) (Figure 6E). In stark contrast to the effects obtained with SAHA and MS-275, the treatment of rats with VPA failed to have any effect on their preference for the social chamber or time spent investigating the stimulus animal ($p=0.3905$; Mann-Whitney U-test) (Figure 6E).

3.6. *CAM-mediated plasticity: Basal and learning-activated NCAM PSA expression*

Given the association of perturbations in NCAM function and ASD (Plioplys et al., 1990; Purcell et al., 2001) and that social cognition deficits are observed in animals lacking the NCAM synapse-specific isoform (Stork et al., 2000) and/or the ability to glycosylate NCAM with polysialic acid (Calandreau et al., 2010), we determined the effect of prior *in utero* exposure to VPA on NCAM PSA expression and plasticity.

Immunohistochemical analysis of hippocampal NCAM PSA in normal animals (VEH/VEH) revealed a discrete population of cells located at the infragranular zone of the dentate gyrus (Figure 7A), as we have described previously in both rodent and human populations (Fox et al., 1995a; Ní Dhuill et al., 1999). These polysialylated cells exhibited established mossy fiber projections and a dendritic arbour that extended into the inner- to mid-molecular layer (Figure 7A). Chronic exposure to SAHA (5 mg/kg), however, resulted in a significant increase of approximately 30% in polysialylated cell frequency ($p=0.03$; Student's t-test). Similarly, chronic exposure to MS-275 (1 mg/kg) also significantly increased polysialylated cell number by approximately 40% ($p=0.0057$; Student's t-test), however, this increase in the basal expression of immunopositive cells was not observed in animals with prior *in utero* exposure to VPA (Figure 7B), suggesting a defective regulation of NCAM glycosylation state.

Given the inability of HDAC inhibition to increase basal numbers of immunopositive cells in VPA-exposed animals, we determined if the learning-induced activation of polysialylated cell frequency, observed at 12 h post-training time following spatial learning (Murphy et al., 1996; Sandi et al., 2004), was also absent. In the vehicle-treated control group (VEH/VEH), the expected significant increase in polysialylated cell frequency was observed at the 12 h post-training time as compared to the passive naïve controls ($p<0.05$; Student's t-test) (Figure 7C). This learning-associated increase in NCAM PSA-immunopositive cells, however, was absent the VPA-treated cohorts (VPA/VEH) indicating these animals to be incapable of mounting a neuroplastic response to the sensory processing demands necessary to consolidate a spatial learning paradigm. Remarkably, chronic treatment of VPA-exposed animals

with MS-275 (1 mg/kg) restored their ability to activate NCAM polysialylation and resulted in the increased polysialylated cell frequency at the 12 h post-training that is necessary for the successful consolidation of the task. It should also be noted that the effect of chronic administration of MS-275 on NCAM PSA was independent of its ability to enhance paradigm acquisition as such learning improvements, as judged by latency to reach the platform, are observed only in the 24 hour and 48 hour training sessions (Figure 5A).

4. DISCUSSION

4.1. *Developmental nature of VPA model of ASD*

The model employed in these studies is based on the premise that *in utero* teratogen exposure alone is sufficient to trigger symptoms of ASD in a neurodevelopmental manner. Crucial to the deployment of this model is the single administration of a large dose of VPA (600 mg/kg) at embryonic day 12 which immediately follows neural tube closure and correlates with brainstem motor nuclei formation. This leads to deficits in the size of these nuclei, the complement of cerebellar neurons, and serotoninergic function; all prominent features of the autistic brain (Rodier et al., 1996; Miyazaki et al., 2005). All offspring of the VPA-exposed dams exhibited a characteristic tail kink that is emblematic of neuralation deficits and the delayed eye-opening observed on postnatal day 14-15 is consistent with abnormalities in the development of motor nuclei controlling the eye muscles (Rodier et al., 1996).

4.2. *Face validity of VPA model of ASD*

Using a standard social approach avoidance paradigm (Brodkin et al., 2004), we now further confirm the observation of robust deficits in social cognition in animals previously exposed to VPA during gestation. As 'approach' is only a single facet of affiliative behaviour, we also determined if deficits in the detection of biological motion existed in the VPA-exposed animals, an important component in multimodal processing of complex social behaviours. We found naïve animals to be readily capable of detecting biological motion, as has been demonstrated previously for rodents (MacKinnon et al., 2010), however the VPA-exposed animals were found to be significantly impaired in this aspect of social perception. These deficits were also

associated with impairments in the water maze paradigm which further indicated that dorsal stream processing was dysfunctional in these animals as spatial learning is reliant on the more dorsal region of the hippocampus (Moser et al., 1993), an area that primarily receives afferents from sensory neocortical regions (Witter and Moser, 2006). Collectively, these observations suggest that prior *in utero* exposure to VPA results in the ontogenetic emergence of a significantly compromised cognitive system that is crucial to normal social behaviour in the adult animal.

Chronic HDAC inhibition reversed the perceptual deficits in adult animals with prior VPA exposure and this was notably evident with MS-275, an inhibitor of HDAC2 (Glaser et al., 2004). Over-expression of HDAC2 has been demonstrated to impair memory formation and, as a consequence, HDAC2 deficiency (Guan et al., 2009) and/or its inhibition with SAHA or MS-275 have cognition-enhancing actions. Further, the ability of SAHA and MS-275 to enhance both spatial learning and social interaction in normal animals suggests that HDAC inhibition directly restores cognitive competence in the VPA-treated animals. The effects of HDAC2 inhibition are likely to be mediated by altered transcription as this isoform is predominantly localised to the nucleus, where it can form stable transcriptional complexes – SIN3A, NuRD and CoReST (Kazantsev and Thompson, 2008). Moreover, the selective localization of HDAC2 to the frontal cortex and hippocampus (Simonini et al., 2006) ensures its inhibition impacts on processing social cognition. Given the impairments in biological motion tasks in autism and their attributions to disruptions in dorsal stream processing (Spencer et al., 2000; Annaz et al., 2012), the deficits observed in these functions in the VPA model of ASD and their drug tractability suggest the

detection of biological motion may be a promising neuroendophenotype to bridge preclinical to clinical drug development initiatives.

4.3. *Construct validity of VPA model of ASD*

Given the association of deficits in NCAM expression and ASD (Plioplys et al., 1990; Purcell et al., 2001), we further sought evidence for construct validity in the VPA rodent model of autism by examining the expression of NCAM PSA and its contribution to the processing of sensory information. The expression of NCAM PSA in the VPA rodent model of ASD revealed a number of unexpected results. In the first instance, there was no difference in the basal frequency of dentate polysialylated neurons between normal and VPA-exposed animals, suggesting the absence of any significant perturbations of structuring in the tightly regulated neurodevelopmental expression of dentate NCAM PSA that is observed in both rodents and humans (Fox et al., 1995b; Ní Dhuill et al., 1999). This lack of effect on basal NCAM PSA expression clearly distinguishes the VPA model of ASD from that of isolation rearing of the Wistar rat, a putative animal model of schizophrenia (Murphy et al., 2010), in which marked deficits in basal hippocampal polysialylated cell frequency are observed (Murphy et al., 2006), as is the case in schizophrenia (Barbeau et al., 1995).

Secondly, animals with prior *in utero* exposure to VPA failed to increase hippocampal polysialylated cell frequency in response to the information demands imposed by spatial learning. This deficit not only confirms the observed inability of VPA-treated animals to acquire and consolidate the water maze paradigm (Murphy et al., 1996; Sandi et al., 2004) but may also be relevant to the social approach avoidance abnormalities that are observed in these animals. NCAM-null mice, for example,

exhibit social deficits manifested by increased aggression, an effect that is counteracted by the introduction of transgenic NCAM180 (Stork et al., 2000), the synapse-specific isoform that carries PSA in adult animals (Persohn et al., 1989; Doyle et al., 1992). Moreover, mice lacking the polysialyltransferase that regulates NCAM PSA in adulthood (PST or ST8SiaIV) also exhibit social deficits and these become even more severe in mice lacking the developmental enzyme (STX or ST8SiaII) (Calandreau et al., 2010). This observation is also of interest in that may the abnormal expression of autism susceptibility genes have been associated with cell adhesion molecules involved in synapse signaling and glycosylation events (Pinto et al., 2010; Ye et al., 2010; Sakai et al., 2011).

Most importantly, however, the activation mechanism for NCAM polysialylation, and ability to acquire the water maze paradigm, is fully restored by treatment with MS-275, an inhibitor of class 1 HDAC isoforms that are involved in memory formation (Guan et al., 2009). In addition, HDAC inhibition is known to enhance NCAM protein expression and the expression of the adult form of polysialyltransferase (PST1) (Lampen et al., 2005). Collectively, these results imply that both the neurobehavioural and neurological deficits induced by *in utero* exposure to the VPA can be reversed in the adult by use of HDAC inhibitors, such as MS-275. Further, it is interesting to note that the deficits induced by *in utero* administration of VPA, which is a HDAC inhibitor (Bolden et al., 2006; Kazantsev and Thompson, 2008), are unrelated to its action in the adult in which it fails to exert any restorative effect on cognitive behaviour. The lack of effect with VPA may, in part, be related to the relative potencies of the inhibitors employed. The IC_{50} for VPA is approximately 400

μM whereas those for SAHA and MS-275 are 70 nM and 11 μM, respectively (Eikel et al., 2006; Beckers et al., 2007).

4.4. *Conclusions*

In these studies, all paradigms employed to interrogate specific aspects of social cognition exhibited significant deficits in the VPA rat model of ASD, a finding we believe provides good face validation of the model. Secondly, the deficits observed in NCAM PSA-mediated plasticity provide compelling construct validity for the model. We have previously demonstrated NCAM turnover to be significantly depressed in individuals with autism (Plioplys et al., 1990) and that this was in direct contrast to the increases observed in schizophrenia (Lyons et al., 1988; see also Tanaka et al., 2009) thereby indicating significant and fundamental differences to exist between the biological constructs of autism and schizophrenia. This may yet provide the unique construct validity necessary to discriminate between animal models of autism and schizophrenia (Tordjman et al., 2007).

5. DISCLOSURE/CONFLICT OF INTEREST

AF is a current employee of Berand Neuropharmacology, AF and CR are members of the Board of Directors for Berand Neuropharmacology. All other authors are past employees of Berand Neuropharmacology. Berand provided financial support for the conduct of the research and in the preparation of the article.

6. LITERATURE CITED

Abrahams BS, Geschwind DH (2010) Connecting genes to brain in the autism spectrum disorders. Arch. Neurol. 67, 395–399.

Alarcon JM, Malleret G, Touzani K, Vronskaya S, Ishii S, Kandel ER, Barco A (2004). Chromatin acetylation, memory, and LTP are impaired in CBP+/- mice: a model for the cognitive deficit in Rubinstein-Taybi syndrome and its amelioration. Neuron 42, 947-959.

American Psychiatric Association (2006) Diagnostic and statistical manual of mental disorders (Revised 4th ed) (DSM-IV-TR) Washington, DC.

Annaz D, Campbell R, Coleman M, Milne E, Swettenham J (2012) Young children with autism spectrum disorder do not preferentially attend to biological motion. J. Autism Dev. Disord. 42, 401-408.

Barbeau D, Liang JJ, Robitalille Y, Quirion R, Srivastava LK (1995) Decreased expression of the embryonic form of the neural cell adhesion molecule in schizophrenic brains. Proc. Natl. Acad. Sci. U.S.A. 92, 2785–2789.

Beckers T, Burkhardt C, Wieland H, Gimmnich P, Ciossek T, Maier T, Sanders K (2007) Distinct pharmacological properties of second generation HDAC inhibitors with the benzamide or hydroxamate head group. Int J Cancer 121, 1138-1148.

Blake R, Shiffrar M (2007) Perception of human motion. Annu. Rev. Psychol. 58, 47-73.

Bolden JE, Peart MJ, Johnstone RW (2006) Anticancer activities of histone deacetylase inhibitors. Nat. Rev. Drug Discovery 5, 769-784.

Brodkin ES, Hagemann A, Nemetski SM, Silver LM (2004) Social approach-avoidance behaviour of inbred mouse strains towards DBA/2 mice. Brain Res. 1002, 151-157.

Bussey TJ, Padain TL, Skillings EA, Winters BD, Morton AJ, Saksida LM (2008) The touchscreen cognitive testing method for rodents: how to get the best out of your rat. Learn. Mem. 15, 516-523.

Calandreau L, Márquez C, Bisaz R, Fantin M, Sandi C (2010) Differential impact of polysialyltransferase ST8SiaII and ST8SiaIV knockout on social interaction and aggresion. Genes Brain Behav. 9, 958-967.

Christianson AL, Chesler N, Kromberg JG (1994) Fetal valproate syndrome: clinical neurodevelopmental features in two sibling pairs. Dev. Med. Child Neurol. 36, 361-369.

Courchesne E, Campbell K, Solso S (2011) Brain growth across the life span in autism: age-specific changes in anatomical pathology. Brain Res. 1380, 138-145.

Doyle E, Bell R, Regan CM (1992) Hippocampal NCAM180 transiently increases sialylation during the acquisition and consolidation of a passive avoidance response in the adult rat. J. Neurosci. Res. 31, 513-523.

Eikel D, Lampen A, Nau H (2006) Teratogenic effects mediated by inhibition of histone deacetylases: evidence from quantitative structure activity relationships of 20 valproic acid derivatives. Chem. Res. Toxicol. 19, 272-278.

Fox GB, O'Connell AW, Murphy KJ, Regan CM (1995a) Memory consolidation induces a transient and time-dependent increase in the frequency of neural cell adhesion molecule polysialylated cells in the adult rat hippocampus. J. Neurochem. 65, 2796-2799.

Fox GB, Kennedy N, Regan CM (1995b). Polysialylated neural cell adhesion molecule expression by neurons and astroglial processes in the rat dentate gyrus declines dramatically with increasing age. Int. J. Dev. Neurosci. 13, 663-672.

Glaser KB, Li J, Pease LJ, Staver MJ, Marcotte PA, Guo J, Frey RR, Garland RB, Heyman HR, Wada CK, Vasudevan A, Michaelides MR, Davidsen SK, Curtin ML (2004) Differential protein acetylation induced by novel histone deacetylase inhibitors. Biochem. Biophys. Res. Commun. 325, 683–690.

Gräff J, Kim D, Dobbin MM, Tsai LH (2011) Epigenetic regulation of gene expression in physiological and pathological brain processes. Physiol. Rev. 91, 603-649.

Guan JS, Haggarty SJ, Giacometti E, Dannenberg JH, Joseph N, Gao J, Nieland TJ, Zhou Y, Wang X, Mazitschek R, Bradner JE, DePinho RA, Jaenisch R, Tsai LH (2009) HDAC2 negatively regulates memory formation and synaptic plasticity. Nature. 459, 55-60.

Ingram JL, Peckham SM, Tisdale B, Rodier PM (2000) Prenatal exposure of rats to valproic acid reproduces the cerebellar anomalies associated with autism. Neurotoxicol Teratol 22, 319-324.

Kazantsev AG, Thompson LM (2008) Therapeutic application of histone deacetylase inhibitors for central nervous system disorders. Nat. Rev. Drug Discov. 7, 854-868.

Kilgore M, Miller CA, Fass DM, Hennig KM, Haggarty SJ, Sweatt JD, Rumbaugh G (2010) Inhibitors of class 1 histone deacetylases reverse contextual memory deficits in a mouse model of Alzheimer's disease. Neuropsychopharmacology 35, 870-880.

Lampen A, Grimaldi PA, Nau H (2005) Modulation of peroxisome proliferator-activated receptor delta activity affects neural cell adhesion molecule and polysialyltransferase ST8SiaIV induction by teratogenic valproic acid analogs in F9 cell differentiation. Mol. Pharmacol. 68, 193-203.

Levenson JM, O'Riordan KJ, Brown KD, Trinh MA, Molfese DL, Sweatt JD (2004) Regulation of histone acetylation during memory formation in the hippocampus. J. Biol. Chem. 279, 40545-40559.

Lyons F, Martin ML, Maguire C, Jackson A, Regan CM, Shelley RK (1988) The expression of a N-CAM serum fragment is positively correlated with severity of negative features in Type II schizophrenia. Biol. Psychiat. 23, 769-775.

MacKinnon LM, Troje NF, Dringenberg HC (2010) Do rats (*Rattus norvegicus*) perceive biological motion? Exp. Brain Res. 205, 571-576.

Maguire EA, Gadian DG, Johnsrude IS, Good CD, Ashburner J, Frackowiak RS, Frith CD (2000) Navigation-related structural change in the hippocampi of taxi drivers. Proc. Natl. Acad. Sci. U.S.A. 97, 4398–4403.

Markram K, Rinaldi T, La Mendola D, Sandi C, Markram H (2008) Abnormal fear conditioning and amygdala processing in an animal model of autism. Neuropsychopharmacology 33, 901-12.

McQuown SC, Barrett RM, Matheos DP, Post RJ, Rogge GA, Alenghat T, Mullican SE, Jones S, Rusche JR, Lazar MA, Wood MA (2011) HDAC3 is a critical negative regulator of long-term memory formation. J. Neurosci. 31, 764-774.

Milne E, Swettenham J, Campbell R (2005) Motion perception and autistic spectrum disorders: A review. Curr. Psychol. Cogn. 23, 3-33.

Miyazaki K, Narita N, Narita M (2005) Maternal administration of thalidomide or valproic acid causes abnormal serotonergic neurons in the offspring: implication for pathogenesis of autism. Int. J. Dev. Neurosci. 23, 287-297.

Moser E, Moser M, Andersen P (1993) Spatial learning impairment parallels the magnitude of dorsal hippocampal lesions, but is hardly present following ventral lesions. J. Neurosci. 13, 3916-3925.

Murphy KJ, O'Connell AW, Regan CM (1996) Repetitive and transient increases in hippocampal neural cell adhesion molecule polysialylation state following multitrial spatial training. J. Neurochem. 67, 1268-1274.

Murphy KJ, ter Horst JPF, Cassidy AW, DeSouza IEJ, Morgunova M, Li C et al. (2010) Temporal dysregulation of cortical gene expression in the isolation reared Wistar rat. J. Neurochem. 113, 601-614.

Murphy KJ, Foley AG, O'Connell AW, Regan CM (2006) Chronic exposure of rats to cognition enhancing drugs produces a neuroplastic response identical to that obtained by complex environment rearing. Neuropsychopharmacology 31, 90-100.

Ní Dhúill CM, Fox GB, Pittock SJ, O'Connell AW, Keith J. Murphy KJ, Regan CM (1999) Polysialylated neural cell adhesion molecule expression in the dentate gyrus of the human hippocampal formation from infancy to old age. J. Neurosci. Res. 55, 99-106.

Paxinos G, Watson C (2007). The Rat Brain in Stereotaxic Coordinates, 6th Ed. Academic Press, New York.

Peça J, Feliciano C, Ting JT, Wang W, Wells MF, Venkatraman TN, Lascola CD, Fu Z, Feng G (2011) Shank3 mutant mice display autistic-like behaviours and striatal dysfunction. Nature 472, 437-442.

Persohn E, Pollerberg GE, Schachner M (1989) Immunoelectron-microscopic localization of the 180 kD component of the neural cell adhesion molecule N-CAM in postsynaptic membranes. J. Comp. Neurol. 288, 92–100.

Pinto D, Pagnamenta AT, Klei L, Anney R, Merico D, Regan R, Conroy J et al. (2010) Functional impact of global rare copy number variation on autism spectrum disorders. Nature 466, 368-372.

Plioplys AV, Hemmens SE, Regan CM (1990) Expression of a neural cell adhesion molecule serum fragment is depressed in autism. J. Neuropsychiat. Clin. Neurosci. 2, 413-417.

Purcell AE, Rocco MM, Lenhart JA, Hyder K, Zimmerman AW, Pevsner J (2001) Assessment of neural cell adhesion molecule (NCAM) in autistic serum and postmortem brain. J. Autism Dev. Disord. 31, 183-194.

Rasalam AD, Hailet H, Williams JH, Moore SJ, Turnpenny PD, Lloyd DJ, Dean JC (2005) Characteristics of fetal anticonvulsant syndrome associated autistic disorder. Dev. Med. Child Neurol. 47, 551-555.

Rodier PM, Ingram JL, Tisdale B, Nelson S, Romano J (1996) Embrylogical origin for autism: developmental anomalies of the cranial nerve motor nuclei. J. Comp. Neurol. 370, 247-61.

Rutherford MD, Troje NF (2011) IQ Predicts Biological Motion Perception in Autism Spectrum Disorders. J. Autism Dev. Disord. [Epub ahead of print].

Sakai Y, Shaw CA, Dawson BC, Dugas DV, Al-Mohtaseb Z, Hill DE, Zoghbi HY (2011) Protein interactome reveals converging molecular pathways among autism disorders. Sci. Transl. Med. 3, 86ra49.

Samaco RC, Neul JL (2011) Complexities of Rett syndrome and MeCP2. J. Neurosci. 31, 7951-7959.

Schneider T, Przewłocki R (2005) Behavioral alterations in rats prenatally exposed to valproic acid: animal model of autism. Neuropsychopharmacology 30, 80-89.

Sandi, C, Cordero MI, Merino JJ, Kruyt ND, Regan CM, Murphy KJ (2004) Neurobiological and endocrine correlates of individual differences in spatial learning ability. Learn. Mem. 11, 244-252.

Silverman JL, Tolu SS, Barkan CL, Crawley JN (2010) Repetitive self-grooming behaviour in the BTBR mouse model of autism is blocked by the mGluR5 anatagonist MPEP. Neuropsychopharmacology. 35, 976-989.

Simonini MV, Camargo LM, Dong E, Maloku E, Veldic M, Costa E, Guidotti A (2006) The benzamide MS-275 is a potent, long-lasting brain region-selective inhibitor of histone deacetylases. Proc. Natl. Acad. Sci. U.S.A. 103, 1587-1592.

Spencer J, O'Brien J, Riggs K, Braddick O, Atkinson J, Wattam-Bell J (2000) Motion processing in autism: evidence for a dorsal stream deficiency. Neuroreport 11, 2765-2767.

Stork O, Welzl H, Wolfer D, Schuster T, Mantei N, Stork S, Hoyer D, Lipp H, Obata K, Schachner M (2000) Recovery of emotional behaviour in neural cell adhesion molecule (NCAM) null mutant mice through transgenic expression of NCAM180. Eur. J. Neurosci. 12, 3291-3306.

Tanaka Y, Yoshida S, Shimada Y, Ueda H, Asai K (2007) Alteration in serum neural cell adhesion molecule in patients of schizophrenia. Hum. Psychopharmacol. 22, 97-102.

Tashiro Y, Oyabu A, Imura Y, Uchida A, Narita N, Narita M (2011) Morphological abnormalities of embryonic cranial nerves after in utero exposure to valproic acid: implications for the pathogenesis of autism with multiple developmental anomalies. Int. J. Dev. Neurosci. 29, 359-364.

Tordjman S, Drapier D, Bonnot O, Graignic R, Fortes S, Cohen D, Millet B, Laurent C, Roubertoux PL (2007) Animal models relevant to schizophrenia and autism: validity and limitations. Behav. Genet. 37, 61-78.

Vallortigara G, Regolin L. Marconato F. (2005) Visually inexperienced chicks exhibit spontaneous preference for biological motion patterns. PLoS Biol. 3, e208.

Vorhees CV (1987) Teratogenicity and developmental toxicity of valproic acid in rats. Teratology 35, 195-202.

Wagner GC, Reuhl KR, Cheh M, McRae P, Halladay AK (2006) A new neurobehvioural model of autism in mice: pre and postnatal exposure to sodium valproate. J. Autism Dev. Disord. 36, 779-793.

Wang et al. (2009) Common genetic variants on 5p14.1 associate with autism spectrum disorders. Nature 459, 528-533

Wegiel J, Kuchna I, Nowicki K, Imaki H, Wegiel J, Marchi E, Ma SY, Chauhan A, Chauhan V, Bobrowicz TW, de Leon M, Louis LA, Cohen IL, London E, Brown WT, Wisniewski T (2010) The neuropathology of autism: defects of neurogenesis and neuronal migration, and dysplastic changes. Acta Neuropathol. 119, 755-770.

Witter MP, Moser EI (2006) Spatial representation and the architecture of the entorhinal cortex. Trends Neurosci. 29, 671-678.

Ye H, Liu J, Wu JY (2010) Cell adhesion molecules and their involvement in autism spectrum disorders. Neurosignals 18, 62-71.

7. FIGURE LEGENDS

Figure 1: Pup early postnatal characteristics following *in utero* exposure to VPA. The characteristic 'tail kink' malformation observed in exposed animals is shown in panel A. Litter size, eye-opening milestone and weight gain parameters are shown in Panel B.

Figure 2: Experimental design employed in establishing the effect of HDAC inhibitors on the social cognition and biological motion deficits observed in the VPA rodent model of autism. The two separate behavioural protocols employed are shown in Panel A. The timeline dimensions are illustrative. The structures of the drugs employed in the protocols are shown in Panel B.

Figure 3: Influence of HDAC inhibitors on the social approach-avoidance deficits in the VPA rodent model of autism. The apparatus employed in the social interaction paradigm is shown in Panel A. The social area shows an experimental animal interacting with the stimulus animal maintained in the chamber. The time spent by the experimental animal in the social, centre and non-social areas is shown in Panel B. All values are the mean$\pm$SEM (n=8) and values significantly different ($p<0.05$) from the control animal (VEH/VEH) are indicated with an asterisk.

Figure 4: Influence of HDAC inhibitors on the biological motion perception deficits in the VPA rodent model of autism. Panel A shows the position of the LCD screen and food magazine at one end of the chamber. The top image to the right shows an

image grab of the 'walking hen' used in the studies and the image below shows a scrambled version of the same. The arrow heads show the direction(s) of motion. The fraction of correct choices for each experimental group over the five daily sessions is shown in Panel B. All values are the mean$\pm$SEM (n=8) and significant differences ($p<0.05$) between the groups (two-way ANOVA) is shown in the Figure.

Figure 5: Influence of HDAC inhibitors on spatial learning deficits in the VPA rodent model of autism. Panel A compares task acquisition rates between control and VPA-treated animals (left) and between VPA-treated animals following administration of HDAC inhibitors SAHA and MS-275 (right). All values are the mean$\pm$SEM (n=8). The influence of gestational exposure to VPA on task recall and the influence of HDAC inhibition on recall deficits is shown in Panel B. All values are the mean$\pm$SEM (n=8) and significant differences ($p<0.05$) between the groups is indicated with an asterisk.

Figure 6: Influence of HDAC inhibitors on spatial learning and social interaction in normal Wistar rats. Panels A, B and C show task acquisition rates between vehicle-treated animals and following chronic administration of HDAC inhibitors SAHA, MS-275 and VPA, respectively. The influence of these HDAC inhibitors on water maze task recall is shown in Panel D. The time spent by control and HDAC inhibitor-treated animals in the social area of the social approach avoidance chamber is shown in Panel E. All values are the mean$\pm$SEM (n=6) and significant differences ($p<0.05$) between the groups is indicated with an asterisk.

Figure 7: Influence of HDAC inhibitors on the frequency NCAM polysialylated cells in the VPA rodent model of autism. The images in Panel A show the distribution of cells at the infragranular zone of the hippocampal dentate gyrus and the increase in their frequency (middle image) and arbour (lower image) following administration of SAHA (5 mg/kg). Quantitative analysis of the NCAM polysialylated cells is shown in Panels A, B, C and D and are the mean$\pm$SEM (n=6). Values significantly different ($p<0.05$) from the controls are indicated with an asterisk. N: Naïve; T: Trained.

A

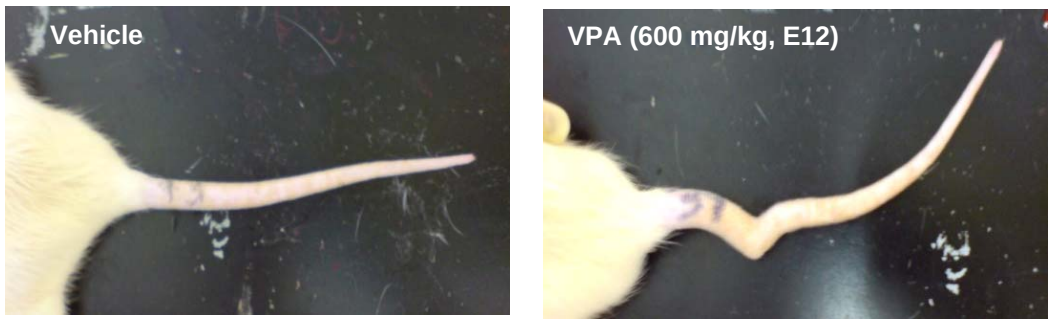

B **Litter characteristics following *in utero* VPA exposure**

	litter size (animal number)			eye opening (postnatal day)	juvenile weight gain (gm; postnatal day 7-16)
	male	female	total		
control	4.8±0.9	5±0.6	9.8±0.4	14.7±0.2	12.5±0.6
VPA-treated	3.9±0.4	4.1±0.9	8±1.0	15.4±0.2*	11.7±0.8

* $P<0.05$, control vs VPA, Student's t-test

Figure 1 Foley et al.

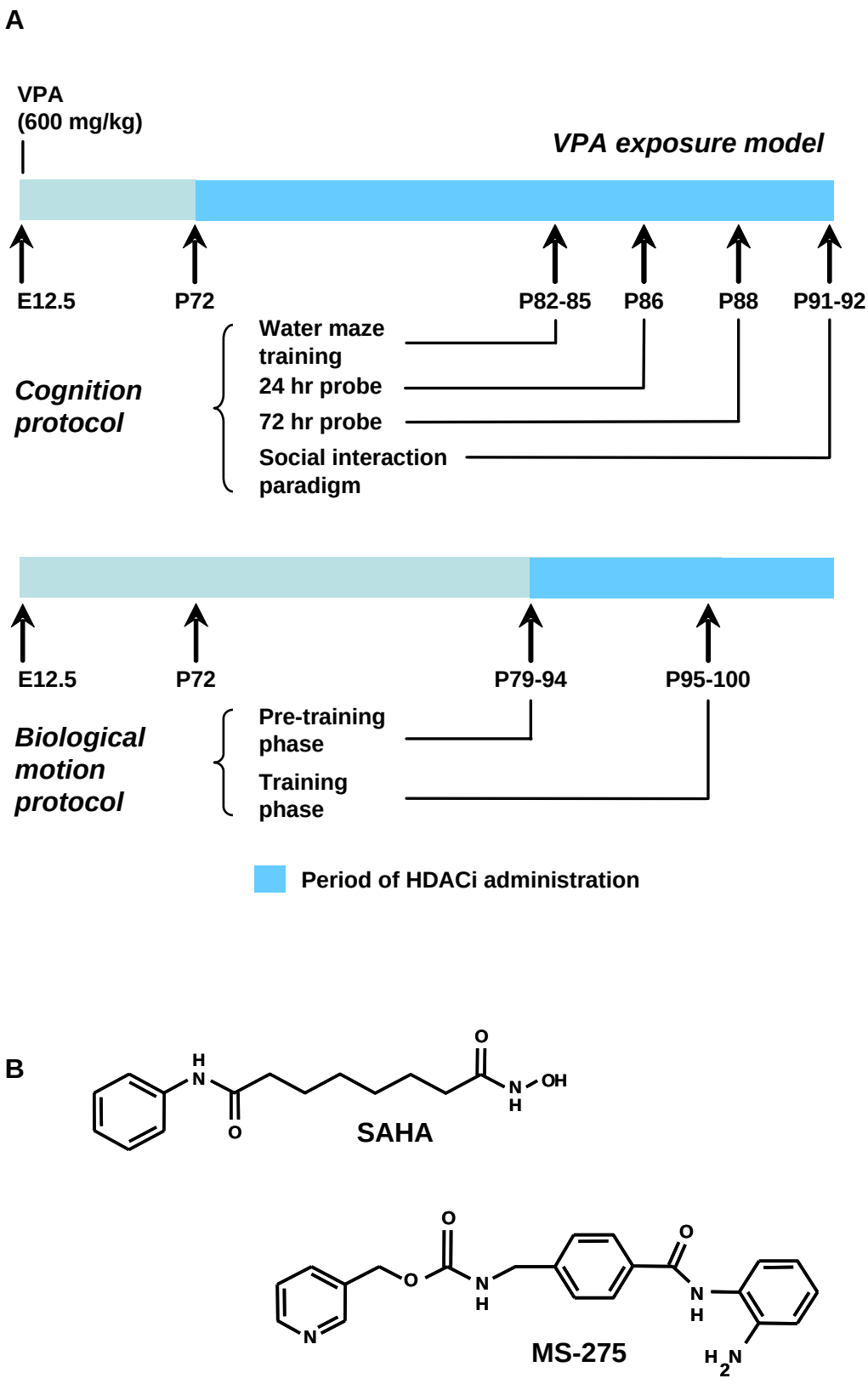

Figure 2 Foley et al.

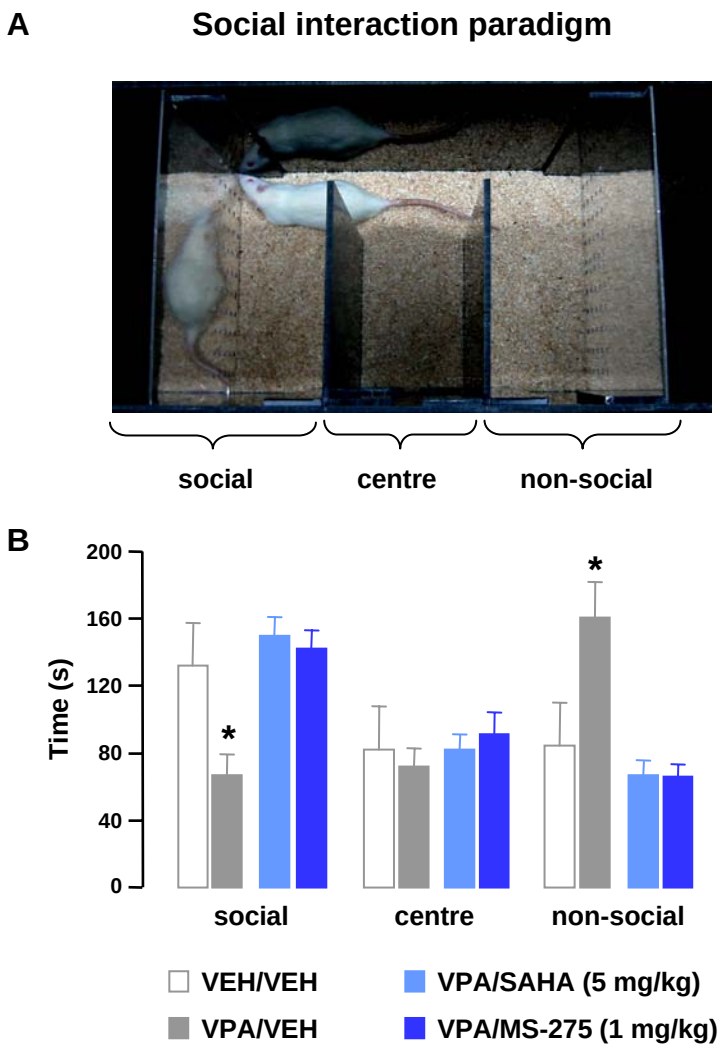

Figure 3 Foley et al.

A **Biological motion perception paradigm**

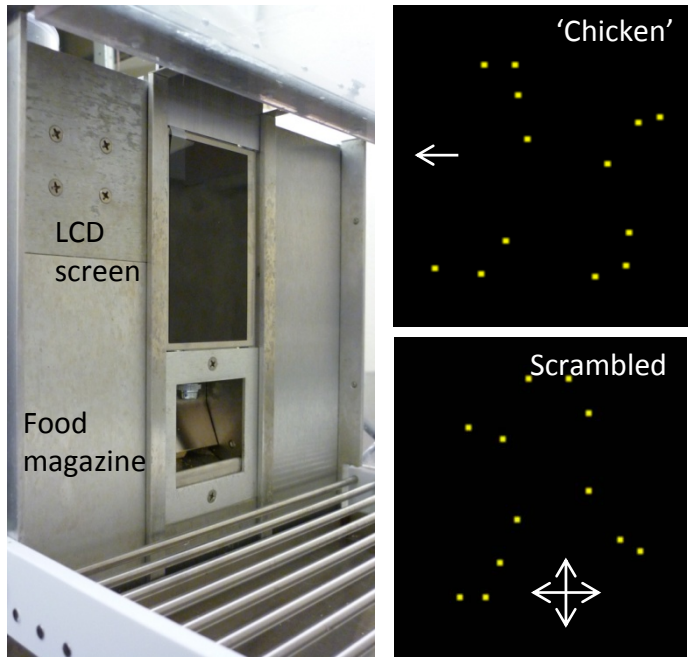

B

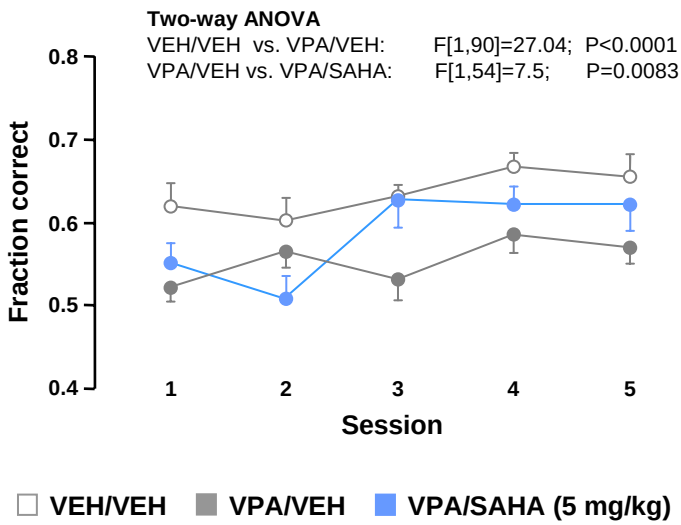

Figure 4 Foley et al.

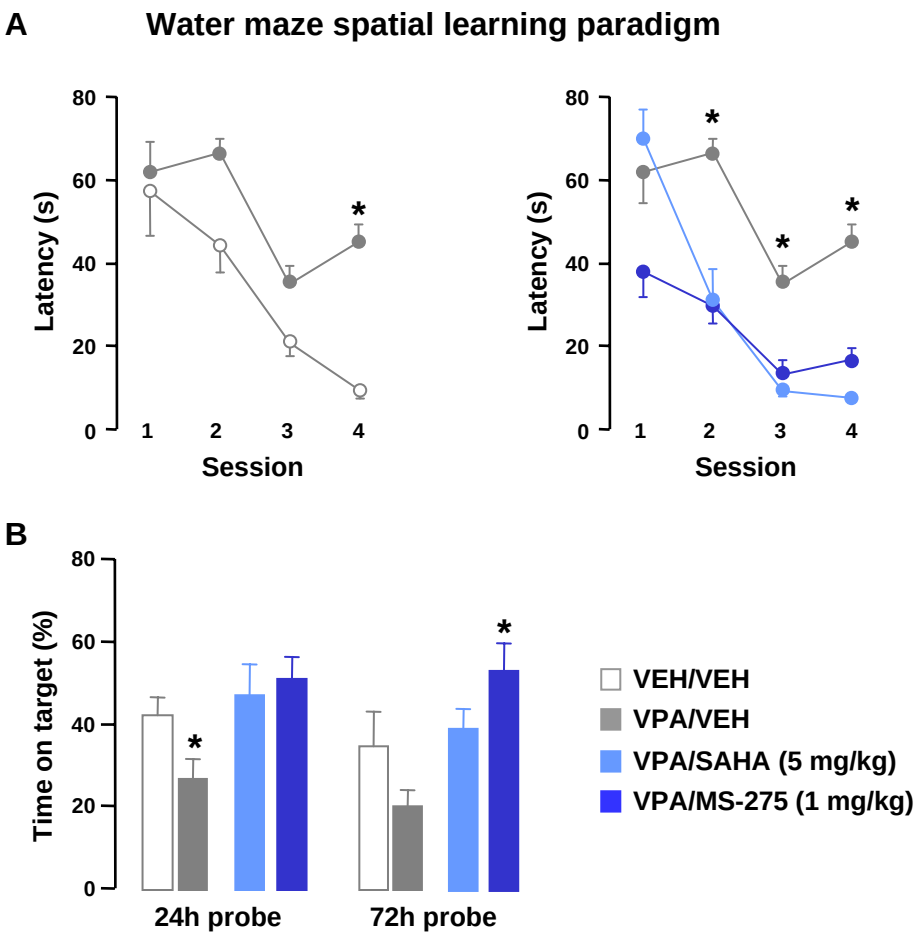

Figure 5 Foley et al.

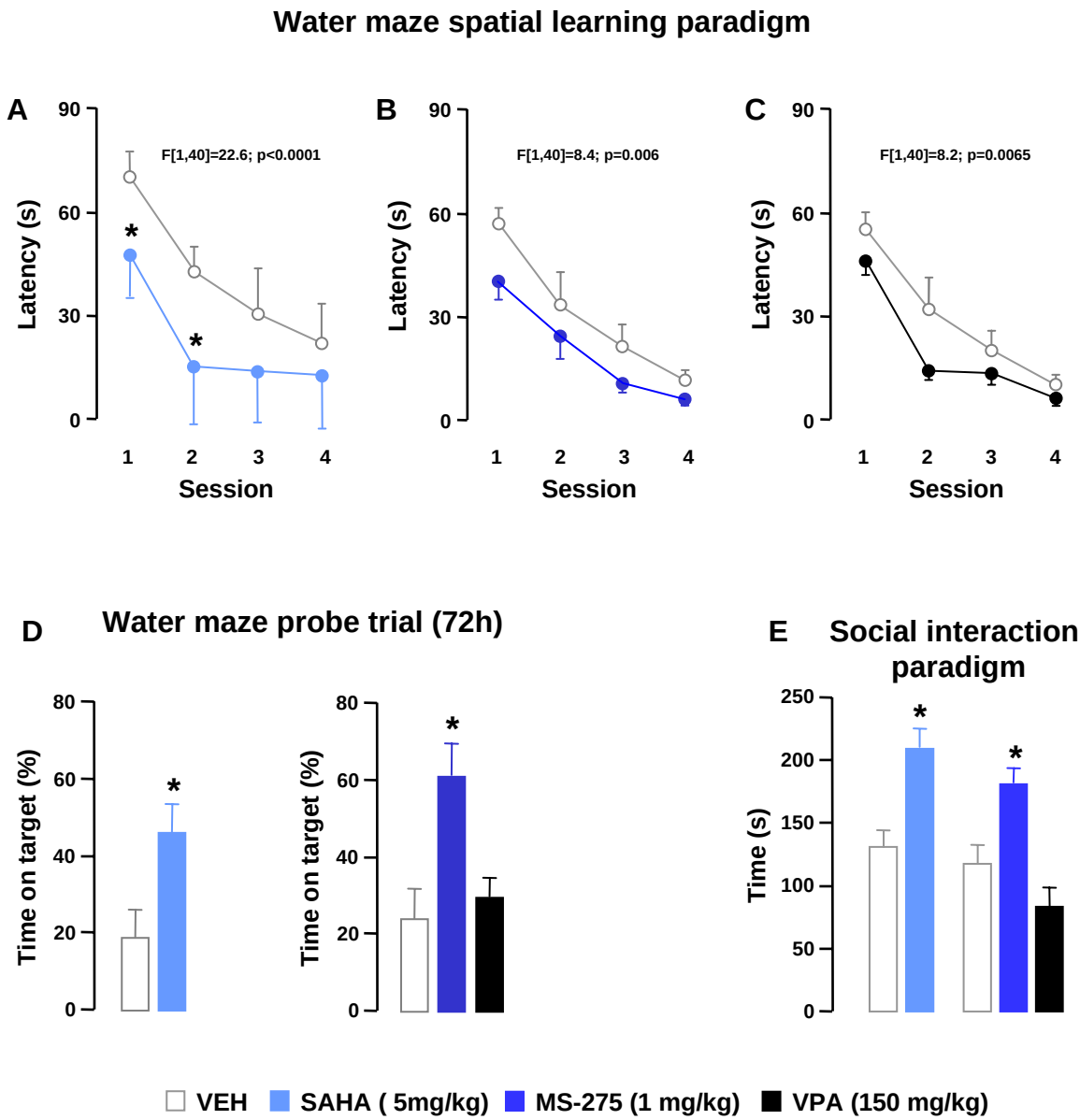

Figure 6 Foley et al.

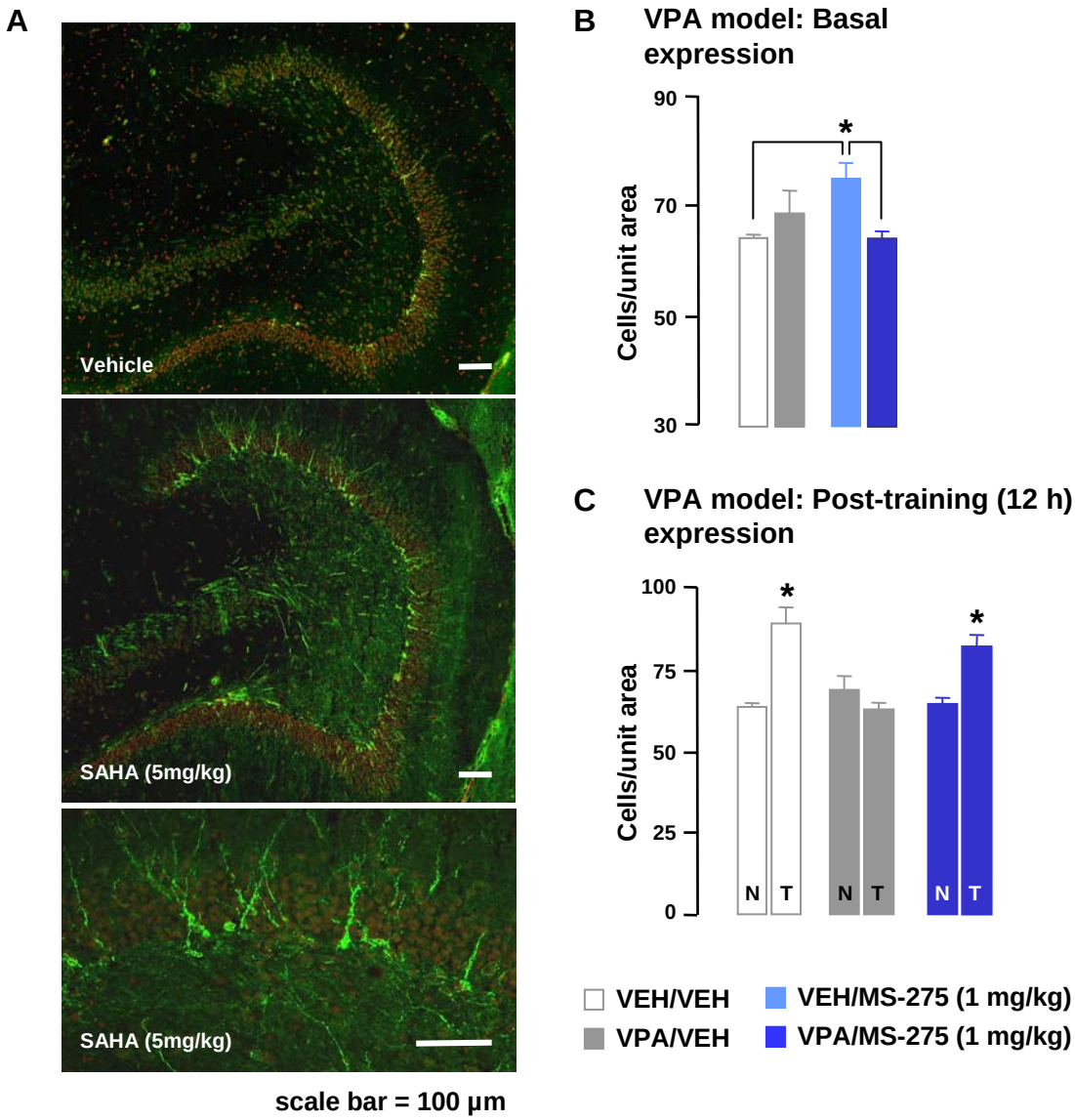

Figure 7 Foley et al.

Table 1. Effect of HDAC inhibition on social behaviour deficits following *in utero* VPA exposure

	social approach-avoidance score	time engaged in social behaviours (sec)
VEH/VEH	47.1±42.0	109.8±6.1
VPA/VEH	-94.4±32.4*	45.4±10.2*
VPA/SAHA	83.6±16.1	107±9.5
VPA/MS-275	76±14.5	113.8±7.4

* P<0.05, vs VEH/VEH, Student's t-test

Table 2. Effect of HDAC inhibition on swim speed and path length in the water maze spatial learning paradigm following *in utero* VPA exposure

	swim speed (cm/s)				path length (m)			
	session 1	**session 2**	**session 3**	**session 4**	**session 1**	**session 2**	**session 3**	**session 4**
VEH/VEH	16.9±1.1	19.4±3.1	19.8±2.3	17.9±1.4	0.99±0.4	0.78±0.3	0.36±0.1	0.13±0.1
VPA/VEH	15.1±1.5	15.8±3.4	16.2±2.5	16.6±1.9	0.94±0.3	1.03±0.3*	0.54±0.3*	0.69±0.3*
VPA/SAHA	16.8±1.2	21.2±2.2	17.0±3.3	19.3±4.1	0.96±0.4	0.66±0.4	0.26±0.1	0.14±0.1
VPA/MS-275	18.5±3.1	17.5±3.4	25.6±3.8	17.7±3.1	0.59±0.3*	0.47±0.2	0.28±0.1	0.26±0.1

* $P<0.05$, vs VEH/VEH, Student's t-test